Web of Scholars: Multidimensional Research Journal
ISSN: 2751-7543
Volume 05 Number 01 (2026)
https://journals.innoscie.com/index.php/wos

Article

Perturbation Effect of Outer Planet on the Orbits of Minor Planets at Different Orbital Elements

Mayada Jasim Hamwdi

1. Department of Electronic and Control Engineering Technologies, Engineering Technical College, Northern technical University, Iraq

* Correspondence: mayadajas@ntu.edu.iq

Abstract: The distribution of a small asteroid 2023 DW minor planet with different eccentricity to the ecliptic plane and with respect to the Jupiter orbit is studied. The variation in orbital elements must be analyzed to effectively study the changes in eccentricity, semi-major axis (SMA), and inclination for the minor planet. The magnitude and direction of these changes depend on the specific conditions, such as the proximity of other bodies and the physical properties of the minor planet. Over time, these forces can significantly alter the orbit, sometimes in predictable ways and sometimes in chaotic or unpredictable patterns.

Keywords: Minor planet, Keplerian orbit, Perturbations, Orbital elements.

Citation: Hamwdi, M. J. Perturbation Effect of Outer Planet on the Orbits of Minor Planets at Different Orbital Elements. Journal of Advanced Research and Scientific Progress 2026, 5(1), 1-9.

Received: 03th Oct 2025
Revised: 18th Nov 2025
Accepted: 24th Dec 2025
Published: 30th Jan 2026

1. Introduction

As defined by the International Astronomical Union (IAU), a minor planet is defined as an astronomical object orbiting the Sun directly and is not classed as a planet or comet. Before 2006, the term "minor planets" was used in the IAU formal classification. During the 2006 IAU General Assembly, however, this classification system was completely scrapped, and new terms like "dwarf planets" were introduced for bodies in these categories. Many asteroids had been identified as dwarf planets by then. One such object was Make-make, which, until 2008, had been called 2005 FY9, but at about 1,200 km across its diameter is five times smaller than Ceres [1]. All minor planets fail to tidy their orbital region, unlike the eight legitimate planets in the Solar System [1], [2]. The object Ceres, which orbits between Mars and Jupiter in the asteroid Belt, was the first to be designated a minor planet. Currently, there are over 100,000 minor planets (asteroids) identified through telescopic observations and measuring methods. Most minor planets have average diameters ranging from 1.52 to 5.20 AU. These small bodies exhibit orbital groupings under the gravitational influence of much larger planets. The first is concentrated in the asteroid belt that lies between Mars and Jupiter, while a smaller number are scattered throughout the rest of our solar system beyond that region. Beyond Saturn's orbit lies the Kuiper Belt, also known as the Edgeworth–Kuiper Belt in honor of its discoverers Kenneth Edgeworth (1880-1972) and Gerard Peter Kuiper (1905-1973) [3].

Ahmed and Mayada analyzed variations in the orbital elements, including the semi-major axis (SMA) (a), eccentricity (e), and inclination (i), to calculate the effects of tides on LEO satellites where studying exoplanetary perturbations is important for understanding the stability of small planets, the motion of transiting objects, and possibly predicting collisions or orbital shifts [4], [5]. Satellites suffer from disturbances due to atmospheric clouds or irregularities in the Earth's gravity, while small planets suffer from disturbances due to the gravitational pull of large planets like Jupiter and Saturn [6].

Theory

Two integration approaches, collocation and multistep, can be used. The program user configures the planetary system, which can comprise all nine planets (or a selection of them) plus one minor planet (an object with insignificant mass) [7], [8].

It is essential to develop robust numerical analysis methods of differential equation systems (DFS) and quadrature mathematics for complex mathematical problems [3].

In any numerical solution of a set of DFS, the error consists not only in the exact solution but also a built-in function known as a numerical approximation. As a result, this makes it difficult for effective integration algorithms to be free of computational errors because they have to assess and control these registration campaigners. However, most difficult of all is how to manage error accumulation and spread when there are so many steps taken in time-based calculations [9], [10], [11].
the orbital elements of a heavenly body and the state vector relating to an arbitrarily picked epoch t:

$$t:\{\boldsymbol{r}(t),\dot{\boldsymbol{r}}(t)\} \leftrightarrow \{a, e, i\ \Omega, w\ T_0\} \dots\dots\dots (1)$$

The osculating orbital elements for the epoch t are defined as

$$t:\{\boldsymbol{r}(t),\dot{\boldsymbol{r}}(t)\} \leftrightarrow \{a(t), e(t)\ i(t)\ \Omega(t), w(t)\ T_0(t)\} \dots\dots\dots (2)$$

t is the osculation epoch, and the osculating elements appearing in relation (2) can be computed by two-body problem relations characteristic for a celestial body under consideration [12].
At epoch t, both the real and osculating Keplerian orbits are tangential.
To focus on the most interesting effects, define the intermediate orbital elements as follows:

$$I(t) \in \{a(t), e(t), i(t), \Omega(t), w(t), T_0(t)\} \dots\dots\dots (3)$$

The average orbital element $\bar{I}(t;\ \Delta t(t))$, averaged over a time period of $\Delta t(t)$ (which can be a function of time in this most general case), is defined as

$$\bar{I}(t;\ \Delta t(t)) = \frac{1}{\Delta t}\int_{t-\Delta t/2}^{t+\Delta t/2} I(t')dt' \dots\dots\dots (4)$$

Given that the osculating elements are continuous functions of time t., equations (3) and (4) define a continuous function of time t. Jupiter's osculating SMA (a) was averaged over a five-revolution period.

$$\Delta t(t) \stackrel{\text{def}}{=} 5P_4(t) \dots\dots\dots (5)$$

$P_4(t)\ =\ (osculating)\ revolution\ period\ of\ Jupiter\ at\ time\ t.$ [13]

Ten time-independent scalar functions of the N-body problem coordinates and velocities have been identified.

In the N-Body problem, there are ten scalar functions of the coordinates and velocities that are known to be time-independent. The amounts are first integers, or simply integers.
Derivative formula for the time development of the system polar moment of inertia. The result is known as the virial theorem [14].
A system of point masses has total angular momentum, which is defined as

$$h \stackrel{\text{def}}{=} \sum_{i=0}^{n} m_i x_i \times \dot{x}_i \dots\dots\dots (6)$$

The whole angular momentum of a system is conserved.

$$\sum_{i=0}^{n} m_i x_i \times \dot{x}_i \stackrel{\text{def}}{=} h \dots\dots\dots (7)$$

The three scalar components of the constant vector h mean that there are three independent first integrals in N-body equations of motion. On the third step, the right represents what happens when you take mean on left and second expressions from course material - step 2. Ultimately one is left with both sides of equation recognizing that they are total time derivatives and hence Energy Conservation Law follows as a matter of course:

$$\frac{1}{2}\sum_{i=0}^{n} m_i \dot{x}^2{}_i - \frac{1}{2}k^2 \sum_{i=0}^{n}\sum_{j=0, j\neq i}^{n} \frac{m_i m_j}{|x_i - x_j|} = E \dots\dots\dots (8)$$

If a point mass is represented by its position vector as sum of the Sun's inertial positive vector and the point mass m_i heliocentric position vector, then minor planets prefer got virgoeric aphelion near Jupiter, In fact, those which have been counted as near Jupilar's farthest point are roughly three times more frequent than those which lie at its periheli where gravity is least and predators lurk in their tentacles. Grouping near Jupiter's perigee has the effect of minimizing the gravitational disturbances each minor planet undergoes when it swings closest to Jupiter. If the minor planets aphelion and Jupiter's aphelion coincide, the minimum distance Δ_{min} between the two bodies fluctuates within the

$$\Delta_{min} = a_4 - a \mp (a_4 e_4 - a\, e) \ldots \ldots \ldots (9)$$

assuming the two orbits are elliptic and coplanar. The minimum distance between the limits differs under the same assumption.

$$\Delta_{min} = a_4 - a \mp (a_4 e_4 + a\, e) \ldots \ldots \ldots (10)$$

if one body's perihelion and the other body's aphelion are the same [15].

2. Materials and Methods

We use a celestial mechanics based numerical and analytical approach to study perturbative effects from the outer planets, especially Jupiter, upon the orbital elements of the minor planet 2023 DW. The methodological framework involves long period numerical integrations of the N-body problem, where the planetary system is modeled to include the dominant planets and a massless minor planet that is gravitationally perturbed. These initial conditions are defined based on osculating Keplerian orbital elements, which in turn focus on changes in eccentricity with a constant semi-major axis. Evolutions of the semi-major axis, eccentricity, inclination, orbital poles and Laplace vector are calculated over simulation time-scales of up to 1 million years, long enough to include both secular and resonant effects. The code works by solving large systems of differential equations that describe orbital motion with numerical integration techniques (embedded quadrature, modified Midpoint Difference (MD) methods solved within the celestial mechanics computational program), while avoiding errors that also accumulate and influence stability in the long-term integrations. We determine time-averaged orbital elements in order to separate short-period oscillations from long-term dynamical behaviours and thereby to obtain a clearer picture of the evolution driven by perturbations. Dynamical systems results are complemented by consideration of vectorial measures like inclination and Laplace vectors, which quantify changes in orbital orientation and precessional behavior as a function of eccentricity. This methodical comparison of results across a wide range of eccentricity cases allows a comprehensive assessment of the impacts of gravitational interactions and resonances on orbital stability, precession and chaos. This integrated numerical–theoretical framework also serves as a foundation for exploring the dynamical development of small bodies under the attracting influence of the outer planets.

3. Results

Figures (1-5) were given the orbital poles for one million years for DW 2023 minor planets at different osculating eccentricities. The change in the orbital poles of a minor planet, especially in relation to its eccentricity (e), is largely governed by gravitational perturbations from other bodies (planets, moons, etc.), as well as by non-gravitational effects. For orbits with low eccentricity (e), the orbital nearly circular, meaning the distance between the object and the Sun does not very much. This leads to relatively stable precession of the orbital pole. For high eccentricity orbits (e), the orbit becomes more elongated, which leads to larger variations in the object's distance from the Sun as it moves along its orbit. This variation has a significant impact on the precision of the orbital pole.

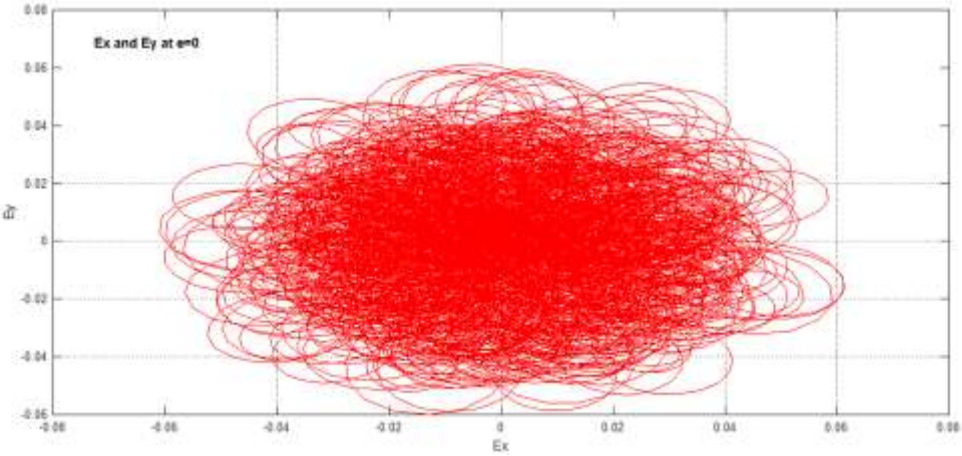

Figure 1. Presents the orbital pole distribution of minor planets having osculating SMA a = 2.497 AU and circular orbits (e = 0.0) throughout the million-year DW 2023 integration timespan**.**

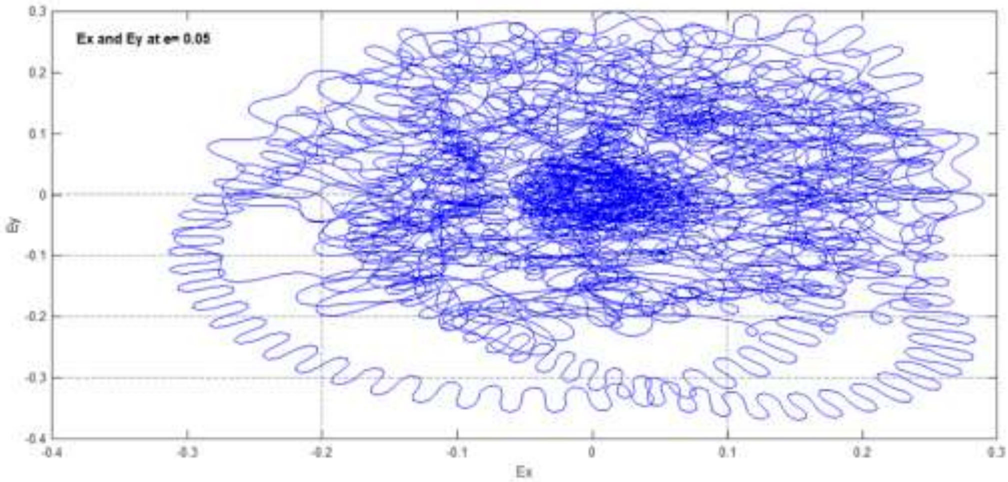

Figure 2. Shows the orbital pole positions of minor planets with SMA $a = 2.497$ AU and eccentricity $e = 0.05$ over the one-million-year DW 2023 simulation period.

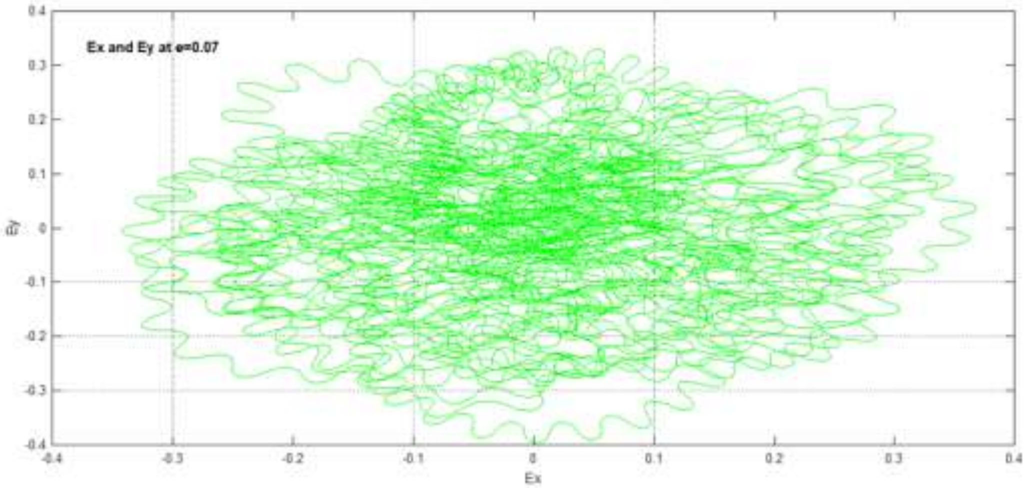

Figure 3. Depicts the poles of orbital in the minor planets characterized by an osculating SMA of 2.497 AU and an osculating eccentricity of 0.07, observed over a one million year period in the DW 2023 dataset.

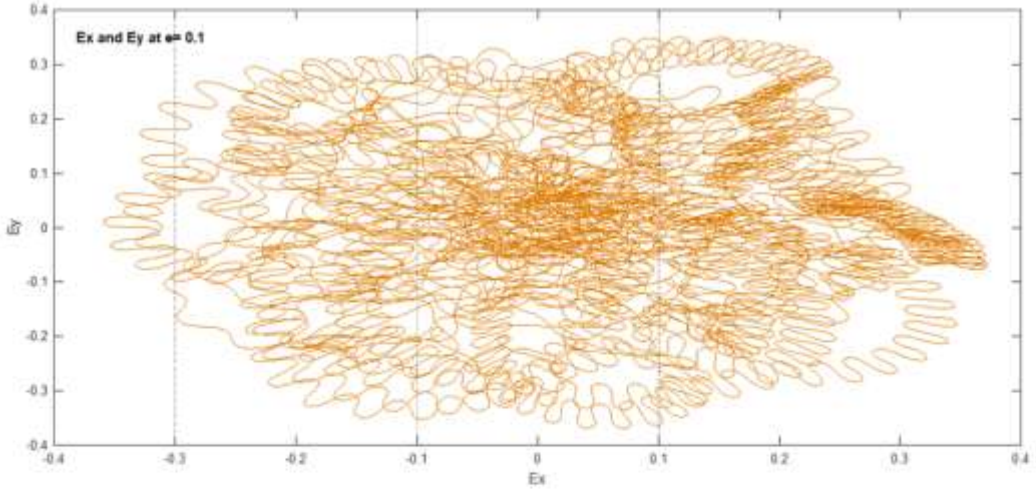

Figure 4. This figure shows the orbital pole positions of minor planets with a SMA of 2.497 AU and an eccentricity of 0.01 over the one-million-year DW 2023 simulation period.

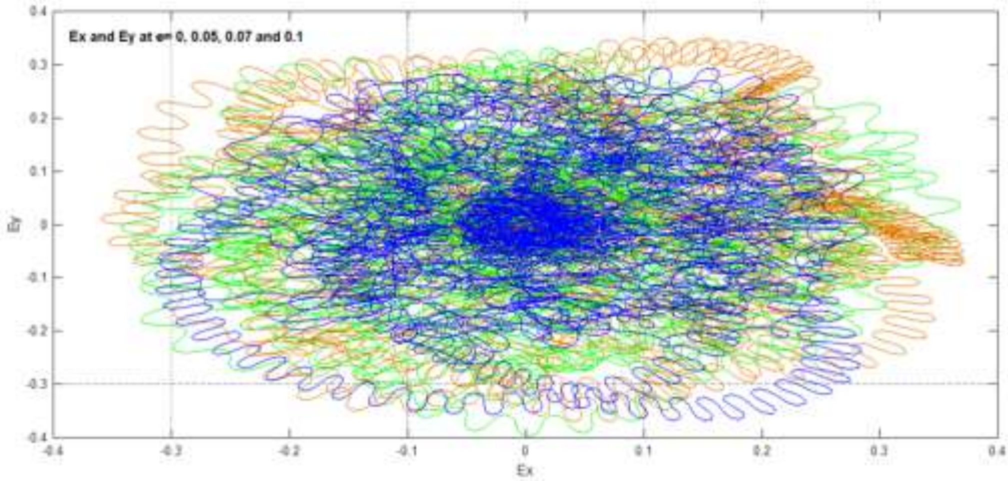

Figure 5. Shows the poles of orbital in the minor planets with osculating SMA a = 2.497 AU and osculating eccentricity e=0.0, 0.05, 0.07 and 0.1 for the one million year DW 2023 period.

Figures 6 through 10 depict DW 2023's Laplace vectors with various eccentricities. At lower eccentricities these will be almost circular in their topside orbit around the origin (x0, y0) = (0, 0) In contrast, a little more distant and prograde orbits lavish instead more markedly elongated projections

The Laplace vector of each minor planet changes dramatically with increasing eccentricity. Low-y (circular) orbit Laplace vectors are stable lines precessed by just a little bit every year or so. For higher eccentricities, gravitational perturbations induced by a slight initial displacement around one point on the equator produce distinct oscillations in time and much greater reforms as an answer: even worse, they grow so strong that cause greater and still faster precession of the vectors.

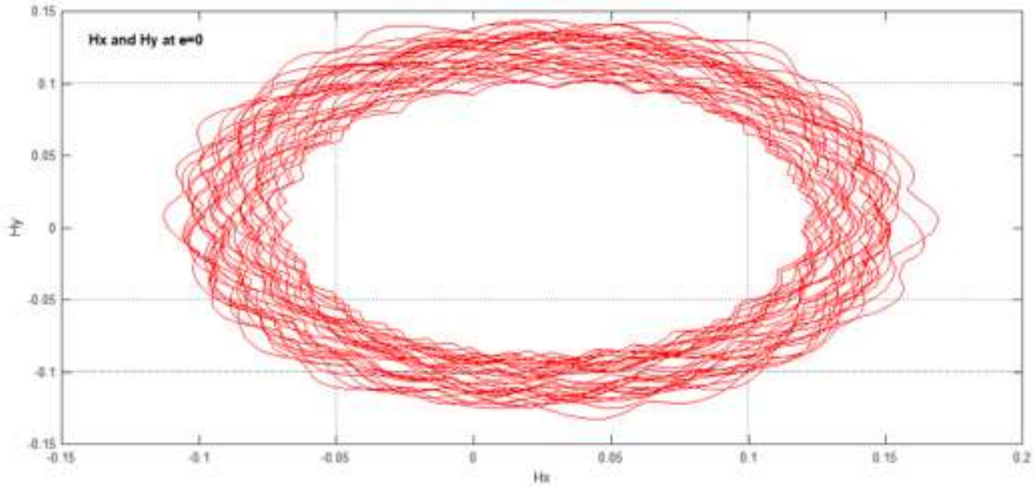

Figure 6. Shows the Laplace vectors of minor planets with osculating SMA $a = 2.497$ AU and osculating eccentricity $e = 0.0$ for the one million year DW 2023 period.

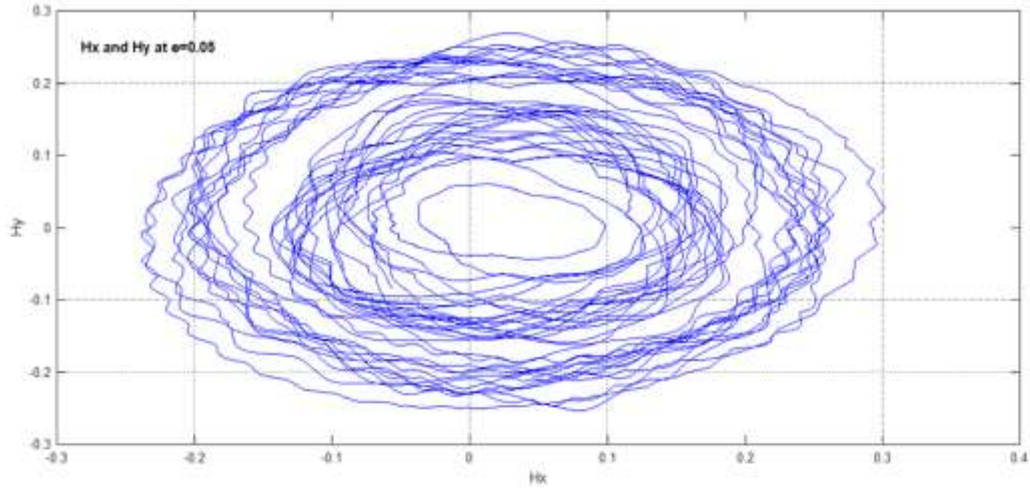

Figure 7. Shows the Laplace vectors of minor planets with osculating SMA a = 2.497 AU and osculating eccentricity e = 0.05 for the one million year DW 2023 period.

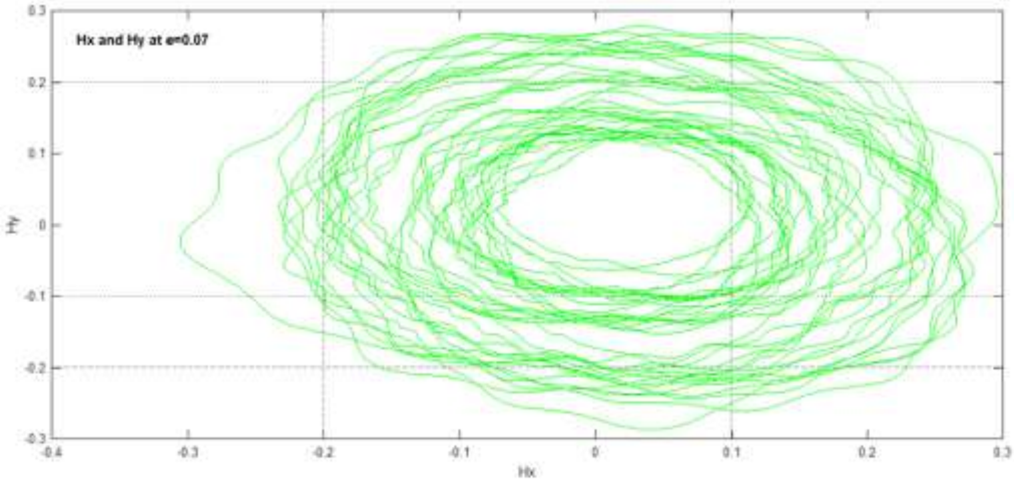

Figure 8. This figure illustrates the Laplace vectors of minor planets with a SMA of 2.497 AU and eccentricity e = 0.07 over the one-million-year DW 2023 simulation period.

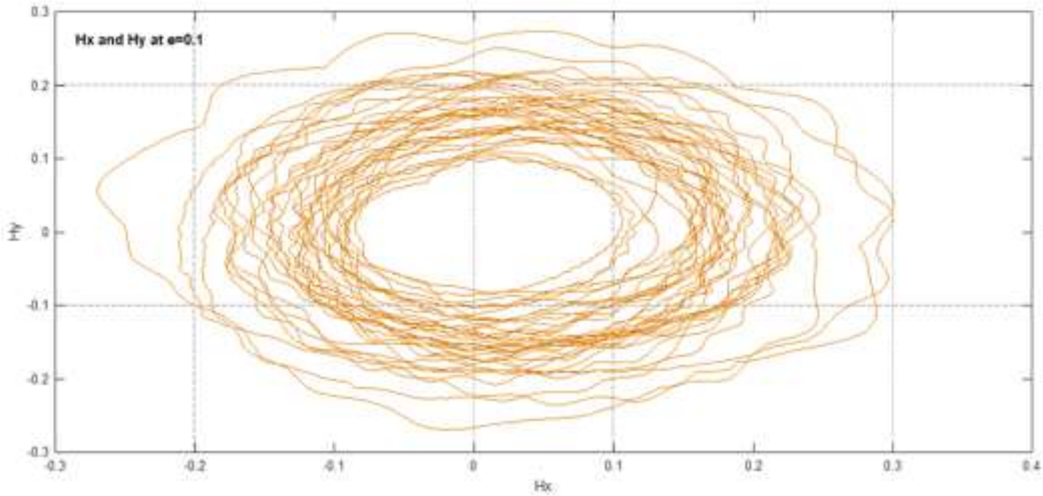

Figure 10. Figure (7) shows the Laplace vectors of minor planets with osculating SMA a = 2.497 AU and osculating eccentricity e = 0.1 for the one million year DW 2023 period.

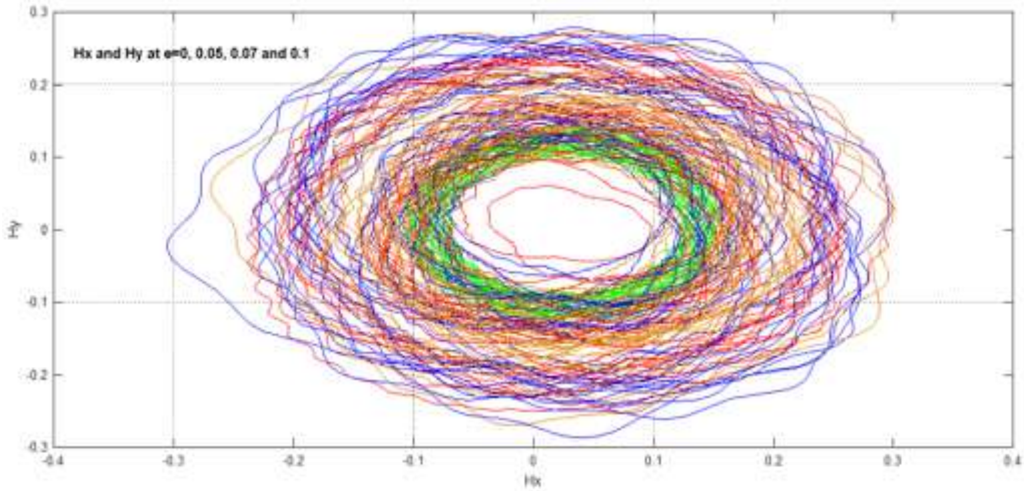

Figure 10. shows the Laplace vectors of minor planets with osculating SMA a = 2.497 AU and osculating eccentricity $e = 0.0, 0.05$, 0.07 and 0.1 for the one million year DW 2023 period

From figure (11) shows the inclination was change as the eccentricity changing as e = 0.0, 0.05, 0.07 and 0.1. The change in inclination computed from the inclination vector, considering the instantaneous rate of change of the inclination over time.

While figure (12) shows the changes in the SMA and eccentricity of a minor planet's orbit are influenced by gravitational perturbations. The magnitude and direction of these changes depend on the specific conditions, such as the proximity of other bodies and the physical properties of the minor planet. Over time, these forces can significantly alter the orbit, sometimes in predictable ways and sometimes in chaotic or unpredictable patterns. Figure (12) shows the changes in the SMA and eccentricity of a minor planet's orbit, these changes can be analyzed under different influences, primarily gravitational interactions, non-gravitational forces, and perturbations. Below is a breakdown of how the SMA and eccentricity of a minor planet can change.

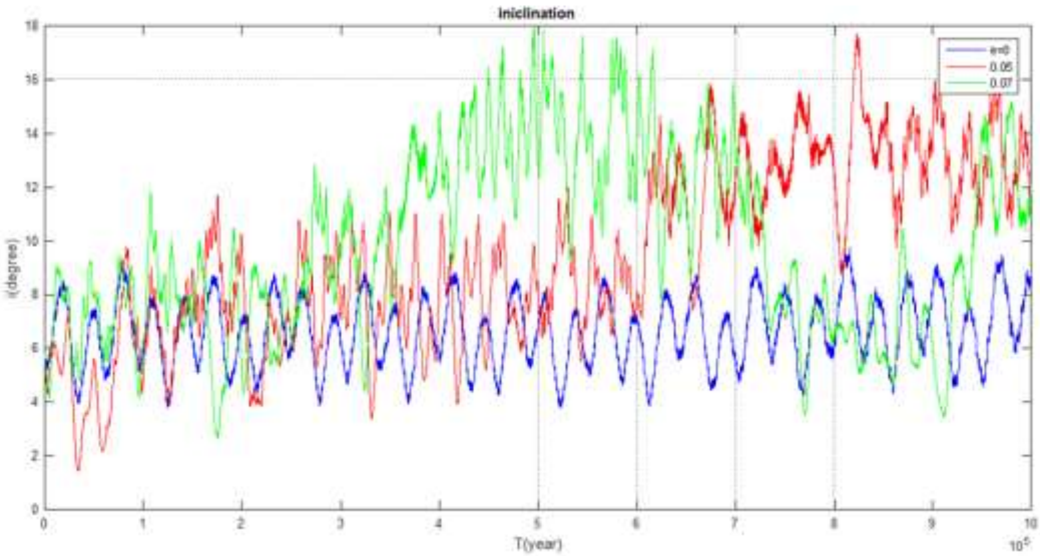

Figure 11. Shows the mean inclination of minor planets over one million years, DW 2023, with an osculating SMA of 2.497 AU and osculating eccentricities of 0.0, 0.05, 0.07, and 0.1, respectively.

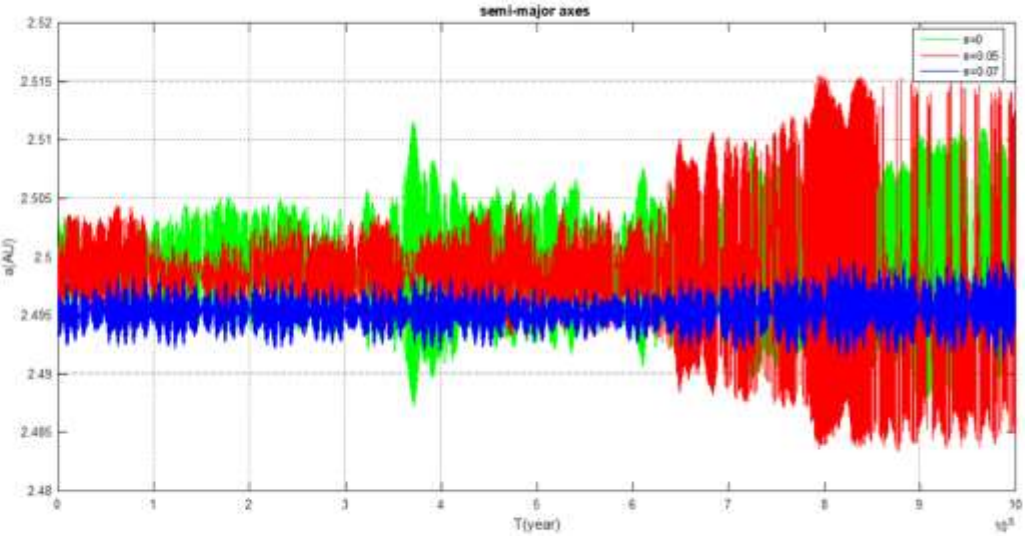

Figure 12. Shows the mean SMA of minor planets over one million years, DW 2023, with an osculating SMA of 2.497 AU and osculating eccentricities of 0.0, 0.05, 0.07, and 0.1, respectively.

The program "celestial mechanics" was employed to find orbits for the minor planet orbit in the planetary system and orbits for satellites or objects orbiting in space. The satellites' study assessed the orbital elements affected by a "perturbing function."

4. Conclusion

The result shows that the orbital evolution of the minor planet 2023 DW is largely controlled by gravitational perturbations which are caused by outer planets but particularly by Jupiter, and the amount and direction of the effects of gravitational perturbations are dramatically changed by small variation of osculating orbital eccentricity value. Orbital poles for minor planets in the low eccentricity region are found to be relatively stable, and Laplace vectors for these minor planets precess slowly and trace elliptical paths, suggesting a significant degree of long term dynamical stability, while trajectories become increasingly chaotic with eccentricity, displaying strong oscillations, accelerated precession and increasing sensitivity to chaotic behavior. We found large differences (up to approximately 10+ degrees) in inclination, semi-major axis, and eccentricity, which indicates the importance of the cumulative effect of both secular and resonant perturbations over the one-million-year integration time. Our results reinforce the reliability of eccentricity as crucial in the amplification of perturbative forces, and consequently, its influence on orbital stability and the long-term dynamical evolution of the asteroid belt. Consequences of this study improve the knowledge of asteroid belt structure, resonance-induced orbital diffusion, and long-term stability analyses of minor planets important for planetary defense and celestial mechanics simulations. In addition, this approach provides additional guidance for perturbation studies in the future: namely, the long numerical integrations and vector-based orbital diagnostics that have been adopted in past work are well-justified as essential methodical framework. More broadly, the analysis could be extended to other minor planets and non-gravitational forces (e.g., Yarkovsky effects), further considering multi-planet resonance interactions and shorter and longer temporal scales to better elucidate the transition from regular to chaotic orbital regimes.

REFERENCES

[1] International Astronomical Union, "IAU 2006 General Assembly: Results of the IAU Resolution votes," Press Release, Aug. 24, 2006. Accessed: May 5, 2008.

[2] International Astronomical Union, "IAU 2006 General Assembly: Resolutions 5 and 6," Aug. 24, 2006. [Online]. Available: https://www.iau.org

[3] A. L. Berger, "Long-term variations of the Earth's orbital elements," *Celestial Mechanics*, vol. 15, pp. 53–74, 1977.

[4] A. K. Izzet, M. J. Hamwdi, and A. T. Jasim, "Analytical study of Earth tides on low-orbit satellites," *Iraqi Journal of Science*, vol. 61, no. 2, pp. 453–461, 2020.

[5] M. J. Hamwdi, "Studying the change in inclination and semi-major axis of satellites for low Earth orbits," *Periodicals of Engineering and Natural Sciences*, vol. 9, no. 2, pp. 500–509, Mar. 2021.

[6] D. D. McCarthy, *IERS Conventions*. Paris, France: Central Bureau of the IERS, Observatoire de Paris, IERS Technical Note No. 21, 1996.

[7] E. M. Standish, "The observational basis for JPL's DE 200, the planetary ephemerides of the Astronomical Almanac," *Astronomy and Astrophysics*, vol. 233, pp. 252–271, 1990.

[8] C. Froeschlé and C. Froeschlé, "Order and chaos in the solar system," in *Proc. 3rd Int. Workshop on Positional Astronomy and Celestial Mechanics*, Cuenca, Spain, Oct. 17–21, 1994, pp. 155–171, A. López García *et al.*, Eds. Valencia, Spain: Universitat de València, Observatorio Astronómico, 1996.

[9] C. D. Murray and S. F. Dermott, *Solar System Dynamics*. Cambridge, U.K.: Cambridge University Press, 1999.

[10] G. Beutler, *Methods of Celestial Mechanics*, vol. II: *Application to Planetary Systems, Geodynamics and Satellite Geodesy*. Berlin, Germany: Springer, 2005.

[11] P. K. Seidelmann, Ed., *Explanatory Supplement to the Astronomical Almanac*. Mill Valley, CA, USA: University Science Books, 1992.

[12] G. Beutler, *Methods of Celestial Mechanics*, vol. I: *Physical, Mathematical, and Numerical Principles*. Berlin, Germany: Springer, 2005.

[13] F. R. Moulton, *An Introduction to Celestial Mechanics*, 2nd rev. ed. New York, NY, USA: Dover Publications, 1970.

[14] N. O. Hasan, W. H. A. Zaki, and A. K. Izzet, "The effect of atmospheric drag force on the elements of low Earth orbital satellites at minimum solar activity," *NeuroQuantology*, vol. 19, no. 9, pp. 24–37, Sep. 2021.

[15] D. A. Vallado, *Fundamentals of Astrodynamics and Applications*, 4th ed. Hawthorne, CA, USA: Microcosm Press, 2013.